PAPER

CrossMark
← click for updates

Comparative studies on the catalytic activity and structure of a Cu-MOF and its precursor for alcoholysis of cyclohexene oxide

Yijiao Jiang,[ad] Jun Huang,*[b] Michael Hunger,[c] Marek Maciejewski[a] and Alfons Baiker[a]

The wide use of metal–organic frameworks (MOFs) in heterogeneous catalysis has been limited due to the fact that the coordination sphere of the metal ions in most known MOF structures is completely blocked by the organic linkers. In this work, a comparative structural study of the precursor $Cu(BF_4)_2 \cdot nH_2O$ (active metal salt catalyst) and the derived Cu-MOF was carried out by using solid-state nuclear magnetic resonance (NMR) and electron paramagnetic resonance (EPR) techniques combined with the study of the interaction of the materials with different reactant molecules by thermogravimetry coupled with mass spectrometry (TG-MS). We clarify how an ideal MOF catalyst can keep the same high reactivity as its metal precursor, and how the existing efficient metal salt/complex catalysts can be linked to analogously reactive MOF catalysts. By choosing proper precursors and organic linkers, MOFs can keep an unsaturated and flexible coordination sphere, which endows them with unique guest-induced reactivity and reactant shape selectivity. The labile coordination facilitates MOFs to perform as well as metal complexes in alcoholysis of cyclohexene oxide but affording good recyclability.

1 Introduction

To date, extensive efforts on the discovery of metal–organic frameworks (MOFs) have afforded a multitude of versatile novel porous materials, which bring emerging applications in various areas such as separation processes, gas storage, membranes and catalysis. This development has been summarized and critically discussed in several reviews.[1–5] Unlike zeolites, carbons and metal oxides, the active metal sites in MOFs are fully exposed and thus provide an ultimately high degree of metal dispersion. In addition, MOFs provide a highly versatile alternative to well-established porous materials by constructing various transition metal nodes and a wide variety of organic bridging ligands with desired functions tailored to a specific application. They allow the design of specific framework geometries with particular pore structure and selective reactivity to reactants.[6–12]

Cyclohexene oxide as a model compound of epoxides is an important intermediate in organic synthesis and the pharmaceutical industry. Alcoholysis of cyclohexene oxide is a widely employed route to undergo ring-opening reactions with nucleophilic species. Due to the very poor nucleophilicity of methanol, the use of strongly acidic or basic conditions is required. The commercially available hydrated copper tetrafluoroborate $(Cu(BF_4)_2 \cdot nH_2O)$ has been employed as an efficient catalyst in ring-opening reactions of epoxides by incorporation of a set of representative alcohols at room temperature.[13] However, the metal salt is toxic, corrosive and environmentally unfriendly. In addition, one of the serious challenges connected with this catalyst is its far better recyclability. To develop more environmentally friendly, safer and cheaper catalytic systems, solid MOF catalysts can open the way to realize the heterogenization of metal salts or complexes, which is of vital importance due to the advantages of simplified recovery and reusability of a green catalyst.[14]

Most existing MOFs are constructed by direct coordination of organic linkers with transition or noble metal ions. The coordination sphere of their precursors is completely saturated, which limits the possibilities of MOFs for catalysis.[12] A few examples of these types of MOFs for applications in catalysis were attributed to structural defects in the MOF materials.[15] We have previously shown the local structural flexibility during adsorption–desorption of reactants on a Cu-MOF composed of copper and 4,4'-bipyridine (bpy) as the

a Institute for Chemical and Bioengineering, ETH Zürich, Hönggerberg, HCI, CH-8093, Zürich, Switzerland
b Laboratory for Catalysis Engineering, School of Chemical and Biomolecular Engineering, The University of Sydney, NSW 2006, Australia. E-mail: jun.huang@sydney.edu.au; Fax: (+61) 2 9351 2854; Tel: (+61) 2 9351 7483
c Institute of Chemical Technology, University of Stuttgart, 70550, Stuttgart, Germany
d Department of Engineering, Macquarie University, NSW 2109, Sydney, Australia

This journal is © The Royal Society of Chemistry 2015

Catal. Sci. Technol., 2015, 5, 897–902 | 897

organic linker, $Cu(bpy)(H_2O)_2(BF_4)_2(bpy)$. The Cu-MOF catalyst has been previously tested in various ring-opening reactions of epoxides with alcohols.[16,17] In the present study, both Cu-MOF and its metal precursor $Cu(BF_4)_2 \cdot nH_2O$ were used as catalysts for alcoholysis of cyclohexene oxide with methanol. Compared to corrosive $Cu(BF_4)_2 \cdot nH_2O$, Cu-MOF exhibited comparable high activity and selectivity but affording good recyclability. Comparative structural studies of Cu-MOF and its precursor $Cu(BF_4)_2 \cdot nH_2O$ were conducted by solid-state NMR, EPR and TG-MS. The results demonstrate that the labile coordination allows the Cu-MOF to keep its flexible local structure in reactions and to provide semi-coordination sites for reactants. Although this work focuses on MOFs, the concept may be also relevant to the design of other catalytic materials.

2 Experimental

Catalyst preparation

Hydrated Cu(II) tetrafluoroborate and 4,4′-bipyridine (98%) were purchased from Aldrich and ABCR Chemicals, respectively. The Cu-MOF was synthesized by addition of an aqueous solution of hydrated copper(II) tetrafluoroborate (0.309 g, 1.0 mmol) to a refluxing ethanol solution of 4,4′-bipyridine (0.312 g, 2.0 mmol).[8,18] A blue precipitate was gradually obtained under stirring. After filtration and washing with water and ethanol, the blue crystals of Cu-MOF were dried at room temperature and then evacuated at 100 °C for 2 h and kept in a glove box. To remove the residual solvents including water and ethanol during the synthesis, the as-synthesized material was dried at 100 °C for 2 h in a Schlenk line and stored under argon. Subsequently, the sample was subjected to an additional evacuation at 100 °C in a vacuum at a pressure of $<10^{-2}$ mbar for 12 h. The vacuumed material was sealed and kept in a glass tube for further use. For the adsorption experiments, the vacuumed sample was loaded with *ca.* 10–30 mbar molecule vapour and then sealed in the glass tubes. Prior to NMR or EPR measurements, the glass tubes were opened in the glove box to avoid water uptake and transferred into a NMR rotor or EPR quartz tube, respectively.

Alcoholysis of cyclohexene oxide with methanol

A suspension containing 1.0 mol% catalyst in 3.2 ml of methanol was added to 2.0 ml of cyclohexene oxide and the reaction was stirred vigorously at room temperature for 10 h. Reaction products were analyzed using an Agilent gas chromatograph equipped with a flame ionization detector (FID) and an HP-5 capillary column. Nonane was used as an internal standard. To confirm the heterogeneity of the reaction, the Cu-MOF was separated from the reaction mixture using a centrifuge (10 000 rpm for 15 min) after 2 h of reaction. For the control experiment, the reaction was stopped after 10 h and the solid catalyst was removed, and the content of Cu ions in the filtrate was analyzed by inductively coupled plasma optical emission spectroscopy (ICP-OES).

Solid-state NMR characterization

All ^1H and ^{11}B magic angle spinning (MAS) NMR studies were performed with a Bruker MSL-400 spectrometer using a 4 mm probe at a spinning rate of *ca.* 8.0 kHz and resonance frequencies of 400.1 and 128.3 MHz, respectively. The spectra were recorded after single pulse excitation with pulse lengths of 2.2 and 1.0 μs, repetition times of 10 and 2 s and accumulation numbers of 80 and 800 for ^1H and ^{11}B nuclei, respectively. The ^1H and ^{11}B MAS NMR spectra were referenced to tetramethylsilane (TMS) and BOSO, respectively.

Continuous-wave (CW) EPR characterization

CW EPR spectra were acquired using a Bruker Elexsys E500 X-Band spectrometer with 30 dB attenuation at room temperature (v_{mw} = 9.865 GHz). Spectral simulations of the CW EPR powder patterns were done using the Matlab package EasySpin.[19]

TG-MS analysis

TG-MS analyses were carried out with a heating rate of 10 °C min^{-1} using an STA 409 analyzer (Mettler). Gases evolved from the decomposition of materials were monitored on-line using an Omnistar (Pfeiffer vacuum) mass spectrometer. The determination of thermal decomposition of Cu-MOF was carried out in He with a flow rate of 50 mL min^{-1}.
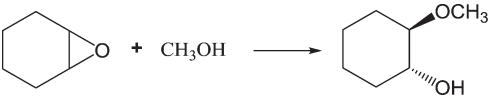
3 Results and discussion

As shown in Scheme 1, the crystalline Cu-based metal–organic framework $Cu(bpy)(H_2O)_2(BF_4)_2(bpy)$ denoted Cu-MOF, which was synthesized by coordinating 4,4′-bipyridine (bpy) with hydrated copper tetrafluoroborate $[Cu(BF_4)_2 \cdot nH_2O]$, comprises both H-bonded bpy and directly coordinated bpy at equatorial positions of a Jahn–Teller elongated Cu(II) octahedron and two BF_4^- anions located axially.[20–22] Table 1 presents the catalytic results of a model ring-opening reaction of epoxides, the alcoholysis of cyclohexene oxide with methanol over $Cu(BF_4)_2 \cdot nH_2O$ and its derived Cu-MOF catalyst. Strikingly, the experimental data demonstrate that with both the Cu metal salt and the Cu-MOF catalysts similar catalytic performance was achieved at room temperature. As a reference catalyst, 2 equiv. of bpy per $Cu(BF_4)_2 \cdot nH_2O$ equivalent to the stoichiometric amount of Cu-MOF (see the second row) was used. With this catalyst the conversion of cyclohexene oxide
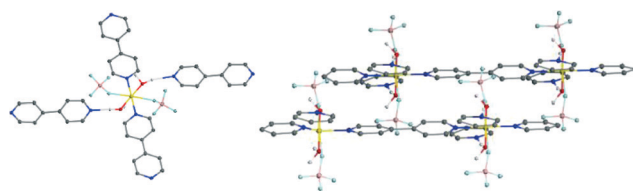
Scheme 1 Coordination geometry of copper(II) centers in the Cu-MOF (a) and view of the 2D sheet of the Cu-MOF (b). C grey, O red, Cu gold, N blue, B pink, F green, and H white.

Table 1 Alcoholysis of cyclohexene oxide with methanol[a]

Catalyst	Conv. (%)	Sel. (%)
$Cu(BF_4)_2 \cdot nH_2O$	98	99
$Cu(BF_4)_2 \cdot nH_2O$ + 2 equiv. bpy	60	87
Cu-MOF	99	99

[a] Reaction conditions: 1 mol% catalyst; ratio of cyclohexene oxide/CH_3OH = 1 : 4; stirred at room temperature for 10 h.

decreased to *ca.* 60% compared to those of the other two catalysts.

To confirm the heterogeneity of the reaction with the Cu-MOF, pertinent control experiments were performed as shown in Fig. 1. After 2 h of the reaction the Cu-MOF was separated from the reaction mixture by a centrifuge (10 000 rpm for 15 min). No significant reaction occurred anymore after removal of the Cu-MOF, indicating that the observed reaction was purely heterogeneous. In another control experiment, the reaction was stopped after 10 h and the solid catalyst was removed. No dissolved Cu ions in the filtrate were detected by ICP-OES, which indicates that leaching of the Cu-MOF catalyst during alcoholysis of cyclohexene oxide was negligible. This behaviour is different from that observed earlier for the alcoholysis of styrene oxide where some leaching of copper was observed which contributed to the reaction by a homogeneous catalytic pathway.[17] This indicates that depending on the solvent and reactant epoxide possible leaching of copper ions and their contribution to the alcoholysis cannot be ruled out.

In Cu-MOF catalysis, a crucial question is how the active sites of the precursor can be accommodated in the coordinated MOF, leading to similar catalytic behaviour of $Cu(BF_4)_2 \cdot nH_2O$ and its derived Cu-MOF. Herein, a comparative study of the precursor $Cu(BF_4)_2 \cdot nH_2O$ (active metal salt catalyst) and the derived Cu-MOF was carried out to clarify whether MOFs could still keep the individual active center of the metal salt during MOF synthesis, whether they exhibit a structure–activity relationship, and how the MOF can maintain the same activity as the metal salt precursor.

Firstly, the formation pathway and persistent nature of active sites from the metal salt $Cu(BF_4)_2 \cdot nH_2O$ to its derived Cu-MOF were investigated by ^{1}H MAS NMR spectroscopy as shown in Fig. 2. Upon evacuation of $Cu(BF_4)_2 \cdot nH_2O$ at room temperature, most of the free water molecules were removed, which led to the ^{1}H NMR spectrum without a signal of bulk water at *ca.* 5 ppm in Fig. 2a. This spectrum shows a dominating signal at *ca.* 0 ppm, *i.e.* at the resonance position of water molecules, which are not involved in hydrogen bonding, but coordinated *via* the oxygen atoms to Cu centers. The high-field shoulders at *ca.* −3 and −6 ppm may indicate that some of the residual water molecules are affected by neighboring BF_4^- anions.

After adding 2 equiv. of bpy to an aqueous $Cu(BF_4)_2$ solution, a new Cu(II) coordination site was generated leading to the formation of the Cu-MOF. Upon subsequent evacuation at room temperature, the ^{1}H MAS NMR spectrum shown in Fig. 2b was recorded. A strong and broad signal at *ca.* 12 ppm appeared due to the protons arising from water molecules coexisting with bpy. The signals between 0 and −6 ppm previously presented in the spectrum of evacuated $Cu(BF_4)_2 \cdot nH_2O$ (Fig. 2a) are covered by the strong signal at *ca.* 12 ppm. The resonance position of this signal is explained by hydrogen bonding between water molecules and bpy in the equatorial plane of the Cu-MOF. Upon further removal of the residual solvent in the Cu-MOF under vacuum at 100 °C for 12 h, the signal of water molecules coordinated to Cu sites appeared again at 0 ppm (Fig. 2c). The peak of the low-field signal, caused by water molecules hydrogen bonded to neighboring bpy, shifted to *ca.* 10 ppm. Quantitative integration of this spectrum gave a ratio of one Cu coordinated water for each
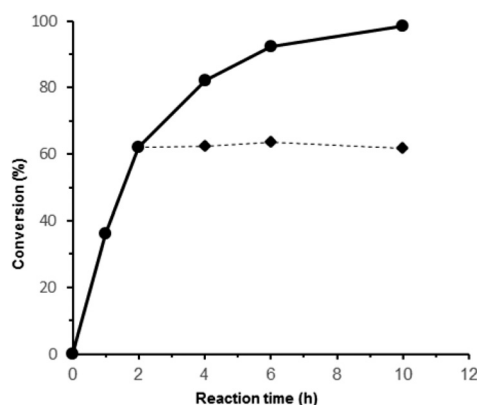

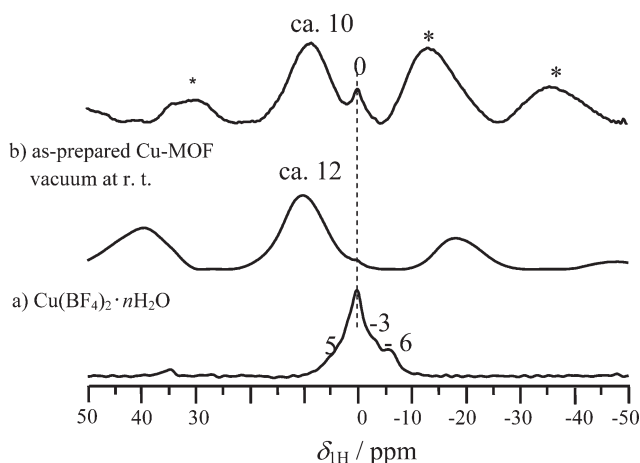**Fig. 1** Heterogeneity test: (●) conversion of cyclohexene oxide in the presence of the Cu-MOF; (♦) no further conversion of cyclohexene oxide was observed after the Cu-MOF catalyst was separated from the reaction mixture after 2 h of the reaction.

Fig. 2 ^{1}H MAS NMR spectra of $Cu(BF_4)_2 \cdot nH_2O$ evacuated at room temperature (a), the as-prepared Cu-MOF evacuated at r. t. (b), and the Cu-MOF evacuated at 100 °C (c). Asterisks denote spinning sidebands.

This journal is © The Royal Society of Chemistry 2015

Catal. Sci. Technol., 2015, **5**, 897–902 | **899**

2 bpy linkers, in good agreement with the stoichiometric amount of water in the Cu-MOF.

Fig. 3 illustrates CW EPR spectra of $Cu(BF_4)_2 \cdot nH_2O$ and Cu-MOF catalysts recorded at room temperature. The EPR spectrum of $Cu(BF_4)_2 \cdot nH_2O$ in Fig. 3a gave $g_\perp$ values typical of six-coordinated Cu species. A qualitatively correct simulation of the spectrum was possible by summing over a species with well-defined g values of 2.054, 2.105 and 2.422 and Lorentzian line-widths of 0.1 mT and a very broad species of $g = 2.060$, 2.130, and 2.428. The comparison of the simulated spectrum to the recorded spectrum indicates the presence of additional and even broader species which might possess similar g values as well. However, values of $g_\perp$ ~2.08 and $g_\parallel$ ~2.42 can be assigned to at least one well-defined species. While the values for $g_\perp$ are typical of six-coordinated Cu(II) species, the very high values found for $g_\parallel$ are rather exceptional and indicate a very weak axial BF_4^- coordination of the Cu centers.

The coordination sphere of the Cu center in the Cu-MOF catalyst is constructed from two directly bonded bpy and two hydrogen-bonded bpy in the equatorial position. The CW EPR spectra of the Cu-MOF (Fig. 3b–c) exhibited typical features of a six-coordinated Cu(II) complex with the lack of resolved Cu hyperfine splitting. The hyperfine interaction was not visible in the spectra, as it was averaged out due to the electron–electron interactions in the Cu-MOF (exchange narrowing). However, the orientation of Cu(II) complexes in the two-dimensional Cu-MOF structure is well defined, and the CW EPR spectra are therefore dominated by well-defined g values which are sensitive to coordination of Cu(II). It seems

that two coordinated water molecules in $Cu(BF_4)_2 \cdot nH_2O$ were replaced with two strong basic bpy molecules during formation of the Cu-MOF, which strongly reduced the Lewis acid strength of the Cu center. Fortunately, the formation of hydrogen bonds between Cu-coordinated water and bpy on the equatorial plane leads to a partial charge transfer and weakens the interaction between the Cu center and the coordinated water, causing unsaturated coordination and reversely an enhanced acidity of this MOF.

However, heretofore it cannot be unambiguously explained why the Cu-MOF has similar reactivity to $Cu(BF_4)_2 \cdot nH_2O$ in reactions. Unlike other rigid porous catalysts, a number of MOFs are known to possess high flexibility of the framework and shrinkage/expansion ability due to interactions with guest molecules.[13,23–26] Our previous results have revealed that chemisorption–desorption of reactants can induce reversible local structural changes of the Cu-MOF.[18] During reversible chemisorption–desorption induced by reactants, there was almost no change in the equatorial coordination of the Cu-MOF. However, a significant change in the axial position was observed. As completely blocked by the organic linkers, the Cu-MOF provides only potential semi-coordination at the axial position. After insertion of bpy ligands, the Cu–Cu distance of the Cu-MOF increased to 11–14 Å.[20–22] Well-distributed Cu centers in the organic framework allow all of them to be accessible to reactants. Metal complexes with ligands offering a flexible framework for molecular catalytic species play a crucial role in achieving high activity and selectivity for many chemical reactions.[27]

In contrast, $Cu(BF_4)_2 \cdot nH_2O$ has four coordinated water molecules in the equatorial position and two BF_4^- anions in the axial position of each Cu center. Upon interacting with electronegative molecules such as CH_3CN, bpy or CH_3OH, both equatorial and axial coordinations were involved in reactions, which might offer less unsaturated coordination for a reactant. As an example, ^{11}B MAS NMR spectra of $Cu(BF_4)_2 \cdot nH_2O$ were recorded before and after adsorption of the probe molecule CH_3CN as shown in Fig. 4. Only part of the Cu centers is available for CH_3CN, and the ^{11}B MAS NMR signal shifted from
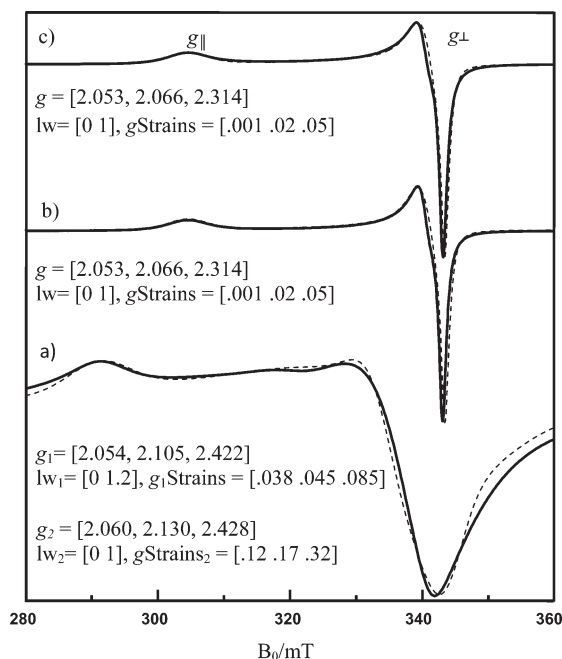

Fig. 3 Room temperature CW EPR spectra of $Cu(BF_4)_2 \cdot nH_2O$ vacuumed at room temperature (a), the as-prepared Cu-MOF (b), and Cu-MOF vacuumed at 373 K (c) and the spectra simulated using with the Cu-MOF samples simulated using the Matlab package EasySpin (dashed line).
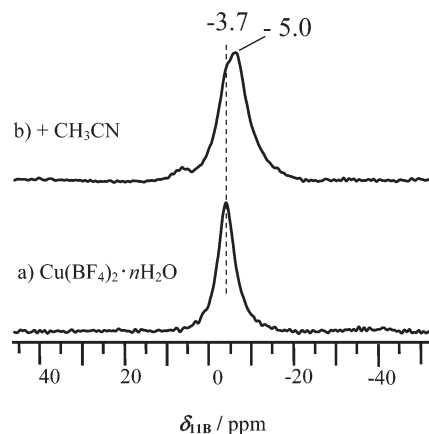

Fig. 4 ^{11}B MAS NMR spectra of vacuumed $Cu(BF_4)_2 \cdot nH_2O$ before (a) and upon loading with CH_3CN (b).

900 | Catal. Sci. Technol., 2015, **5**, 897–902

This journal is © The Royal Society of Chemistry 2015

−3.7 to −5.0 ppm. This finding indicates that the interaction between Cu centers and fluorine arising from BF_4^- became weaker due to the interactions of CH_3CN with Cu active sites in both cases. A high-field shift of $\Delta\delta_{11B} = -1.3$ ppm is obtained for $Cu(BF_4)_2 \cdot nH_2O$, but $\Delta\delta_{11B} = -3.8$ ppm for the Cu-MOF.[18] It means that the Cu–F bonds became much weaker in the Cu-MOF, which leads to more unsaturated coordination Cu sites for reactions. It might be one of the reasons that the Cu-MOF exhibits the same high reactivity as $Cu(BF_4)_2 \cdot nH_2O$, although the Cu-MOF possesses less Lewis acidity compared to its precursor $Cu(BF_4)_2 \cdot nH_2O$. This is also one reason that a mixed compound of 2 equiv. of bpy per $Cu(BF_4)_2 \cdot nH_2O$ exhibited very poor reactivity (Table 1, second row). This knowledge could be of vital importance for the rational design of MOF catalysts.

It is clear that the structural flexibility of $Cu(BF_4)_2 \cdot nH_2O$ and Cu-MOF can be traced back to a Cu coordination change, which plays a crucial role in the catalytic performance of both MOF and its precursor. The Cu-MOF is expected to have flexible and unsaturated coordination for reactants, which allows continuation of the reaction process and avoidance of blocking the reaction by a very rigid coordination. Motivated by this, combined thermogravimetric and mass spectrometric investigations (TG-MS) were carried out for analysing the desorption temperatures of various reactants interacting with Cu-MOF active sites. The experiments were carried out on the samples containing only water (as-prepared Cu-MOF), only methanol (loaded on Cu-MOF after removal of water at 100 °C in vacuum $<10^{-2}$ mbar) and both species (after loading with CH_3OH followed by sample rehydration). The MS signals depicting the evolution of species adsorbed on active Cu sites are presented in Fig. 5 for water (a) and methanol (b). As shown in Fig. 5a, the maximum of water evolution from the as-prepared Cu-MOF is centered at 182 °C. In the presence of CH_3OH, this maximum shifts to a lower temperature of 159 °C. This finding indicates that in the presence of CH_3OH, the coordination between water and Cu-MOF became weaker.

In contrast, the results presented in Fig. 5b indicate the influence of water on the interaction of CH_3OH with the Cu-MOF. In the Cu-MOF sample containing only methanol, the maximum desorption rate is observed at 230 °C. Upon rehydration of the CH_3OH-containing Cu-MOF, the temperature of this maximum significantly decreased from

230 °C to 167 °C, which indicates a strong weakening of the coordination between CH_3OH and Cu-MOF in the presence of water. These results support the hypothesis that the Cu-MOF exhibits labile unsaturated active sites for reactants. When a reactant molecule is activated by these unsaturated Cu sites for reaction, the interaction of the reactant with Cu sites can be weakened and even replaced with another reactant molecule to continue the reaction.

One should keep in mind that not all of the reactants can induce a coordination change and initiate the reaction over the Cu-MOF. Polar and non-polar molecules were chosen to study the coordination change. For polar molecules, such as acetone and pyridine, the obvious coordination changes between Cu and BF_4^- ions were detected by ^{11}B MAS NMR spectroscopy as shown in Fig. 6. After adsorption of acetone on the vacuumed Cu-MOF, the ^{11}B MAS NMR signal obviously shifted from −2.0 to −5.3 ppm, which is due to the weakening binding between Cu(ii) and fluorine arising from BF_4^-. These coordination changes were found to correlate well with the electric dipole moments of the polar molecules as summarized in Table 2. A higher electric dipole moment of the model molecule leads to a stronger interaction with the Cu center to produce much weaker Cu–F bonds, which provide more unsaturated sites for reactants and reversely enhance the reactivity of the Cu-MOF.

Apparently, the ^{11}B MAS NMR spectra in Fig. 6d–e showing no high-field shift of boron atoms were obtained after introducing non-polar molecules, such as n-butane, and even smaller molecules, such as carbon monoxide (CO). It implies that these non-polar molecules were not able to induce the unsaturated coordination sites and open the gate for reactions themselves, but polar molecules can do so. This
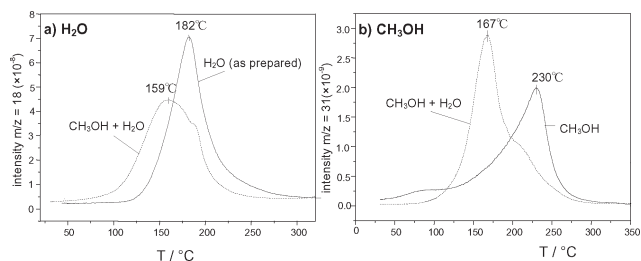

Fig. 6 ^{11}B MAS NMR spectra of Cu-MOF (a), loaded with acetone (b), pyridine (c), CO (d), and n-butane (e).

Fig. 5 Mass spectrometric signals of water (a) and methanol (b) evolved during TA-MS measurements from Cu-MOF samples containing one or both (dashed line) species chemisorbed on the active Cu sites.
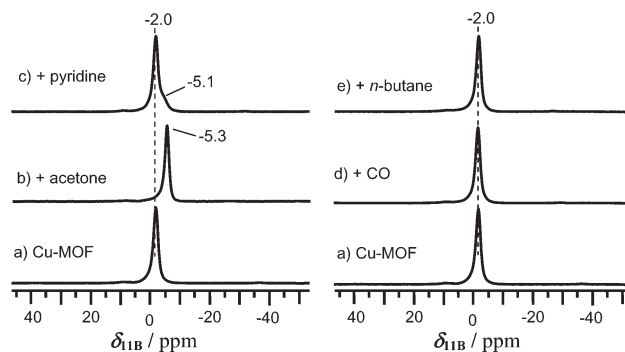
Table 2 Correlation between electric dipole moments of reactants and high-field chemical shifts ($\Delta\delta_{11B}$)

Reactants	Electric dipole moment[28]	$\Delta\delta_{11B}$
Methanol	1.70	2.9 (ref. 18)
Pyridine	2.19	3.1
Acetone	2.88	3.3
Acetonitrile	3.92	3.8

phenomenon gives a hint that the Cu-MOF exhibits unprecedented guest-induced reactivity to generate semi-coordinated Cu sites in reactions. This leads Cu-MOF to maintain virtually the same activity as its metal salt. However, the reactivity of the Cu-MOF cannot be enhanced by a coordination change in the reactions with non-polar reactants.

It is important to note that the reactant shape selectivity, which is one key property of zeolites,[29] was obviously observed for the Cu-MOF in this work. For relatively small polar molecules, such as acetone, CH_3CN, and CH_3OH, all Cu centers in the MOF were accessible and caused high-field shifts of all BF_4^- signals in the ^{11}B MAS NMR spectra. However, pyridine cannot enter and interact with Cu sites due to its large molecular size. As shown in Fig. 6c, pyridine molecules were only adsorbed on the outer Cu sites and resulted in a small shoulder at ca. −5.1 ppm, even under much higher pyridine vapour pressure (60 mbar) than that for the abovementioned smaller molecules. As reported previously,[22] the Cu-MOF consists of the quasi-square grid 2D layered stacking structure. The square grid framework has dimensions of 1.13 nm × 1.15 nm, and the distance between neighboring layers is only 0.46 nm, whilst the molecular diameter of pyridine is 0.60 nm.[30] Thus, it is understandable that pyridine cannot access the Cu sites in the Cu-MOF structure. From this observation, tuning of the cavity diameter of the Cu-MOF by selecting organic linkers with different sizes should allow controlling the reaction process to obtain the desired products.

Conclusions

This work clarified how an ideal MOF catalyst keeps the same high reactivity as its metal precursor, and how the existing efficient metal salt/complex catalysts can be linked to analogously reactive MOF catalysts. By choosing appropriate precursors and organic linkers, MOFs can keep an unsaturated and flexible coordination state, which makes them perform as well as metal complexes in reactions. In addition, the Cu-MOF has been shown to exhibit guest-induced reactivity and reactant shape selectivity. These findings may help in bringing the development of MOF catalysts to a more rational design.

Acknowledgements

Notes and references

1 A. Corma, H. García and F. X. Llabrés i Xamena, Chem. Rev., 2010, 110, 4606–4655.
2 D. Farrusseng, S. Aguado and C. Pinel, Angew. Chem., Int. Ed., 2009, 48, 7502–7513.
3 G. Ferey, Chem. Soc. Rev., 2008, 37, 191–214.
4 A. M. Shultz, O. K. Farha, J. T. Hupp and S. T. Nguyen, J. Am. Chem. Soc., 2009, 131, 4204–4205.
5 M. Ranocchiari and J. A. V. Bokhoven, Phys. Chem. Chem. Phys., 2011, 13, 6388–6396.
6 Y.-H. Yeom and H. Frei, J. Phys. Chem. A, 2001, 105, 5334–5339.
7 R.-Q. Zou, H. Sakurai and Q. Xu, Angew. Chem., Int. Ed., 2006, 45, 2542–2546.
8 C.-D. Wu, A. Hu, L. Zhang and W. Lin, J. Am. Chem. Soc., 2005, 127, 8940–8941.
9 F. X. Llabrés i Xamena, O. Casanova, R. Galiasso Tailleur, H. Garcia and A. Corma, J. Catal., 2008, 255, 220–227.
10 S. Hermes, M.-K. Schröter, R. Schmid, L. Khodeir, M. Muhler, A. Tissler, R. W. Fischer and R. A. Fischer, Angew. Chem., Int. Ed., 2005, 44, 6237–6241.
11 M. Sabo, A. Henschel, H. Frode, E. Klemm and S. Kaskel, J. Mater. Chem., 2007, 17, 3827–3832.
12 X. Zhang, F. X. Llabrés i Xamena and A. Corma, J. Catal., 2009, 265, 155–160.
13 J. Barluenga, H. Vázquez-Villa, A. Ballesteros and J. M. González, Org. Lett., 2002, 4, 2817–2819.
14 I. Luz, F. X. Llabrés i Xamena and A. Corma, J. Catal., 2010, 276, 134–140.
15 U. Ravon, M. E. Domine, C. Gaudillere, A. Desmartin-Chomel and D. Farrusseng, New J. Chem., 2008, 32, 937–940.
16 D. Jiang, T. Mallat, F. Krumeich and A. Baiker, J. Catal., 2008, 257, 390–395.
17 D. Jiang, A. Urakawa, M. Yulikov, T. Mallat, G. Jeschke and A. Baiker, Chem. – Eur. J., 2009, 15, 12255–12262.
18 Y. Jiang, J. Huang, B. Kasumaj, G. Jeschke, M. Hunger, T. Mallat and A. Baiker, J. Am. Chem. Soc., 2009, 131, 2058–2059.
19 S. Stoll and A. Schweiger, J. Magn. Reson., 2006, 178, 42–55.
20 A. J. Blake, S. J. Hill, P. Hubberstey and W.-S. Li, J. Chem. Soc., Dalton Trans., 1998, 909–916.
21 D. Li and K. Kaneko, Chem. Phys. Lett., 2001, 335, 50–56.
22 A. Kondo, H. Noguchi, S. Ohnishi, H. Kajiro, A. Tohdoh, Y. Hattori, W.-C. Xu, H. Tanaka, H. Kanoh and K. Kaneko, Nano Lett., 2006, 6, 2581–2584.
23 X. Zhao, B. Xiao, A. J. Fletcher, K. M. Thomas, D. Bradshaw and M. J. Rosseinsky, Science, 2004, 306, 1012–1015.
24 R. Matsuda, R. Kitaura, S. Kitagawa, Y. Kubota, T. C. Kobayashi, S. Horike and M. Takata, J. Am. Chem. Soc., 2004, 126, 14063–14070.
25 K. Biradha, Y. Hongo and M. Fujita, Angew. Chem., Int. Ed., 2002, 41, 3395–3398.
26 P. L. Llewellyn, G. Maurin, T. Devic, S. Loera-Serna, N. Rosenbach, C. Serre, S. Bourrelly, P. Horcajada, Y. Filinchuk and G. R. Férey, J. Am. Chem. Soc., 2008, 130, 12808–12814.
27 P. Sautet and F. Delbecq, Chem. Rev., 2009, 110, 1788–1806.
28 D. R. L. R. D. Nelson and A. A. Maryott, in Handbook of Chemistry and Physics, ed. R. C. West, CRC Press, Cleveland, Ohio, 56th edn, 1975, pp. E63–E65.
29 B. Smit and T. L. M. Maesen, Nature, 2008, 451, 671–678.
30 A. Satsuma, D. Yang and K. Shimuzu, Microporous Mesoporous Mater., 2011, 141, 20–25.